Appl Biochem Biotechnol (2012) 166:889–902
DOI 10.1007/s12010-011-9478-6

The Construction of Glucose Biosensor Based on Platinum Nanoclusters—Multiwalled Carbon Nanotubes Nanocomposites

Cheng Yan Wang · Xing Rong Tan · Shi Hong Chen · Fang Xin Hu · Hua An Zhong · Yu Zhang

Received: 5 October 2011 / Accepted: 29 November 2011 /
Published online: 4 January 2012

Abstract One-step synthesis method was proposed to obtain the nanocomposites of platinum nanoclusters and multiwalled carbon nanotubes (PtNCs–MWNTs), which were used as a novel immobilization matrix for the enzyme to fabricate glucose biosensor. The fabrication process of the biosensor was characterized by cyclic voltammetry, electrochemical impedance spectroscopy, atomic force microscopy and scanning electron microscope. Due to the favorable characteristic of PtNCs–MWNTs nanocomposites, the biosensor exhibited good characteristics, such as wide linear range (3.0 μM–12.1 mM), low detection limit (1.0 μM), high sensitivity (12.8 μA mM^{-1}), rapid response time (within 6 s). The apparent Michaelis–Menten constant (K_m^{app}) is 2.1 mM. The performance of the resulting biosensor is more prominent than that of most of the reported glucose biosensors. Furthermore, it was demonstrated that this biosensor can be used for the assay of glucose in human serum samples.

Keywords Biosensor · Platinum nanoclusters · Multiwalled carbon nanotubes · Nanocomposites · Glucose oxidase

Introduction

Glucose is a key metabolite for living organisms, particularly in the case of patients bothered by diabetes [1]. As a clinical indicator of diabetes, the glucose sensor has played a principal role in the move of simple one-step blood sugar testing and continuous real-time glucose monitoring. In addition, it is also a kind of tool in food industry and environmental analysis [2]. As a result, there is an ever-growing demand to create the sensitive, reliable, recyclable and low-cost glucose sensors [3].Turbidity sensors [4], viscometric affinity sensors [5], piezoelectric sensors [6, 7], surface plasmon resonance based sensors [8] and electrochemical biosensors [9] have

C. Y. Wang · S. H. Chen (✉) · F. X. Hu · H. A. Zhong · Y. Zhang
Key Lab of Chongqing Modern Analytical Chemistry, Education Ministry Key Laboratory on Luminescence and Real-Time Analysis, College of Chemistry and Chemical Engineering, Southwest University, Chongqing 400715, China
e-mail: cshong@swu.edu.cn

X. R. Tan
Department of Endocrinology, 9th People's Hospital of Chongqing, Chongqing 400700, China

been extensively studied. Based on the simplicity, rapid response, high sensitivity and low cost, the electrochemical biosensors can be a good choice for glucose measurement. To the electrochemical biosensors, enzymatic glucose electrochemical biosensors are of particular importance due to the biospecific affinity of enzyme for its substrate [10].

Recent researches indicate that the properties of catalysts could be ameliorated by changing the grain size, texture and the surface profile of the catalysts. Thus, the research for producing nanosized material to enhance its activity is a critical theme in the analysis and catalysis research areas [11]. Various nanomaterials, such as nanoparticles, nanoclusters, nanotubes, nanorods, nanobelts and nanoislands have been universally used as immobilization matrix or catalyst for the construction of electrochemical sensing and biosensing devices with favorable analytical performances, thanks to their large surface-to-volume ratios and increased surface activities [12, 13]. Particularly, the transition-metal nanoclusters, consisting of less than about a few hundreds of atoms, open a promising field toward the development of the biosensor since they have significant potential as new types of higher activity and selectivity catalysts [14]. Transition-metal nanoclusters are widely used to enhance the performances of electrodes because of their huge surface area and high catalytic activity. Li et al. [15] fabricated a reagentless amperometric cancer antigen 15–3 immunosensor based on the direct electrochemistry of glucose oxidase with carbon nanotubes (CNTs) and platinum nanoclusters (PtNCs) as an electron relay. The cooperation of CNTs and PtNCs increased the sensitivity of the immunosensors. Zhao [16] et al. constructed a novel amperometric biosensor based on ZnO:Co nanoclusters for biosensing glucose. Due to the high specific active sites and high electrocatalytic activity of the ZnO:Co nanoclusters, the constructed glucose biosensor showed a high sensitivity.

However, the aggregation of nanoclusters often makes such electrodes prone to poisoning or corrosion, and prohibits their applications in the construction of biosensor [17]. To overcome this problem, various forms of carbon are commonly used as electrode materials to support the metallic catalysts [18]. CNTs, as a new form of carbon materials discovered by Iijimain 1991 [19], are the first choice since they possess special properties, such as huge surface area, excellent electronic performance and good biocompatibility [20]. The combination of metal nanoclusters and CNTs not only prohibits the aggregation of the nanoclusters but also improve the performances of electrodes. Ishikawa et al. [21] realized the rapid and label-free cell detection with Cr and Au cluster-decorated CNTs biosensors, and the sensitivity of biosensors with the clusters had been enhanced by 2,000-folds and the detection of streptavidin was down to 10 pM concentration.

It's reported that some researchers have constructed platinum nanoparticles–carbon nanotubes (PtNPs–CNTs) composites modified electrodes via physisorbing presynthesized PtNPs on CNTs [22], or via electrodeposition of PtNPs with Pt salt solution on CNTs [23, 24]. However, physisorbed PtNPs are prone to remove by agitating the composites in liquid and then formed Pt agglomeration [25], and electrodeposition of PtNPs is possibly concurrent reduction of H^+ [26]. We now propose the PtNCs–MWNTs nanocomposites films obtained by the method of one-step synthesis as a new alternative for the immobilization of glucose oxidase (GOX). The performance of the prepared glucose biosensor with respect to linear range, detection limit and sensitivity is presented and discussed. The proposed strategy for constructing the biosensor is ground on the following advantages: first of all, the size-uniform PtNCs could be decorated on the surface of MWNTs stably via one-step synthesis, and the preparation process is very simple and realizable. Secondly, the combination of PtNCs and MWNTs made the PtNCs–MWNTs composites possess eminent properties, such as large surface-to-volume ratio, favorable electrical conductivity, high catalytic activity and good biocompatibility, thus, leading to a high sensitivity for the glucose detection at the biosensor. Thirdly, the preparation of the biosensor is easy, which means to shorten the

period of biosensor construction and reduce the cost of per assay. Thus, the biosensor has good application potential in glucose detection.

Experimental

Reagents and Materials

Multiwalled carbon nanotubes (MWNTs >95% purity), chloroplatinic acid ($H_2PtCl_6 \cdot 6H_2O$), GOX, D-(+)-glucose (99.5%), H_2O_2 (30%) and Nafion (5 wt.% solution in lower aliphatic alcohol) were purchased from Sigma(St. Louis, MO, USA). $K_3[Fe(CN)_6]$, $K_4[Fe(CN)_6]$, KCl, NaOH, formaldehyde, N,N-Dimethyformamide and ethylene glycol was purchased from Chongqing Chuandong chemical regent company (Chongqing, China). Phosphate buffer solutions (PBS) with various pH values were prepared with H_3PO_4 and NaOH solution and the supporting electrolyte was 0.1 M KCl. All other chemicals were of analytical grade and used without further purification. A stock solution of 5.0 mg mL^{-1} GOX was prepared with 0.1 M PBS (pH 7.0). Double-distilled water was used throughout this study.

Apparatus and Measurements

Electrochemical impedance spectroscopy (EIS) measurements were carried out with a Model IM6e (ZAHNER Elektrick Co., Germany) in the presence of 5.0 mM $K_3[Fe(CN)_6]/K_4[Fe(CN)_6]$ (1:1) mixture as a redox probe. The alternative voltage was 5 mV and the frequency range was 50 mHz–10 kHz. Electrochemical measurements were carried out on CHI 660D electrochemical work station (Shanghai CH Instruments Co., China) in a three-electrode electrochemical cell containing a platinum wire auxiliary electrode, a modified glassy carbon electrode (GCE) as working electrode and a saturated calomel electrode as reference electrode against which all potentials were measured. The test solutions were 5.0 mL 0.1 M PBS. All the electrochemical experiments were carried out at room temperament.

Scanning electron micrographs were taken with a scanning electron microscope (SEM, Hitachi Co., Japan). Atomic force microscopy (AFM) images of the films were achieved by scanning probe microscope (Vecco, USA).

Preparation of PtNCs–MWNTs

PtNCs–MWNTs nanocomposites were prepared according to the reference [27] with a slight modification. For the synthesis of PtNCs–MWNTs composites, the MWNTs (5 mg) were suspended and stirred in 5 mL ethylene glycol and then 1 mL of 1% H_2PtCl_6 solution was added in the above solution. A 1.0 M NaOH solution was added to adjust pH of the solution to about 11. Formaldehyde aqueous solution was added to reduce Pt at 90 °C for 2 h, and then heated at 140 °C for 3 h for a complete reduction of Pt. The solid was centrifuged and washed with double-distilled water and then dried at 70 °C in the vacuum.

Modification of the Electrode

The GCE (Φ=4 mm) was carefully polished with alumina slurry (grain size, 0.3 and 0.05 μm) until a mirror was obtained. Subsequently, to remove the alumina residues from the electrode surface, ultrasonic rinsing with ethanol and water was necessary. Such prepared electrode was dried for the modification.

To fabricate a PtNCs–MWNTs nanocomposites-modified electrode, 2 mg of PtNCs–MWNTs were dispersed into 1 mL double-distilled water to obtain 2 mg mL^{-1} PtNCs–MWNTs suspension with the aid of ultrasonic. Then, 5 μL of the suspension was modified onto the surface of pretreated GCE with a micro-syringe and the solvent was allowed to evaporate at the ambient temperature. To construct the enzyme electrode, 5 μL GOX (5 mg mL^{-1}) was cast onto the PtNCs–MWNTs/GCE. After drying in refrigerate, the electrode was covered by 2 μL of Nafion (1 %) to prevent possible enzyme leakage and eliminate foreign interferences. The solvent was allowed to evaporate before use. The final electrode is taken as the Nafion/GOX/PtNCs–MWNTs/GCE. The similar procedures were employed to fabricate the Nafion/GOX/MWNTs/GCE excepted that pure MWNTs were dispersed into 1 mL N,N-Dimethyformamide. All resulting electrodes were stored at 4 °C when not in use. The procedure for preparing glucose biosensor is schematically shown in Scheme 1.

Results and Discussion

SEM and AFM Characterizations of the Biosensor

The surface morphologies of the PtNCs–MWNTs and PtNCs–MWNTs/GOX films were investigated with SEM and the images are shown in Fig. 1. The image of the PtNCs–MWNTs nanocomposites shows that the PtNCs have an average size of 10 nm and are distributed randomly on the surface of MWNTs (Fig. 1a). When GOX were assembled onto the films of PtNCs–MWNTs composites (Fig. 1b), the tubiform structure of the PtNCs–MWNTs become blurry, indicating that GOX biomolecules were immobilized successfully on the surface of electrodes.

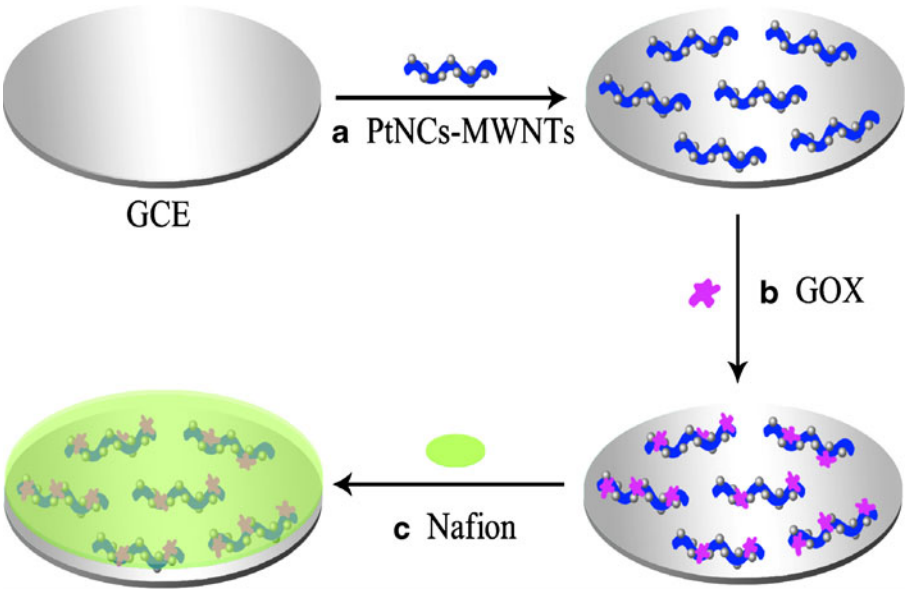

Scheme 1 The illustration of the preparation process of Nafion/GOX/PtNCs–MWNTs/GCE

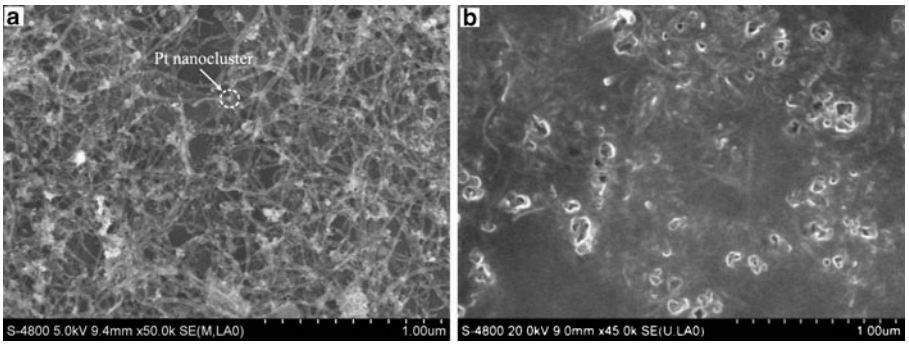

Fig. 1 SEM images of the PtNCs–MWNTs films (**a**) and GOX/PtNCs–MWNTs films (**b**)

To further confirm the surface morphologies of the modified films, AFM technology was employed. Figure 2 illustrates the typical AFM images of the PtNCs–MWNTs and PtNCs–MWNTs/GOX films-modified gold surface. As showed in the Fig. 2a, on the surface of the gold substrate, many tubiform substances are present clearly, and the PtNCs also could be observed on the surface of the tubiform structure, which is ascribed to the successful assembly of the PtNCs–MWNTs. Its root mean square (RMS) roughness is 58.7 nm. The AFM image of the PtNCs–MWNTs/GOX films (Fig. 2b) exhibits a smoothing effect with the diminished RMS roughness (27.3 nm) as compared to that of the PtNCs–MWNTs films, which might be due to GOX molecules filling the interstitial places between the PtNCs–MWNTs composites.

Electrochemical Characterization of the Biosensor

To probe the interface features of the modified electrodes, the method of EIS was applied. The value of electron transfer resistance (R_{et}) depends on the dielectric and insulating features at the electrode/electrolyte interface. Figure 3a shows the impedance features of different modified electrodes in the presence of 5.0 mM $K_3[Fe(CN)_6]/K_4[Fe(CN)_6]$. The R_{et} for a bare GCE was estimated to be 143 Ω (curve a) and a sharp decrease for the R_{et} value

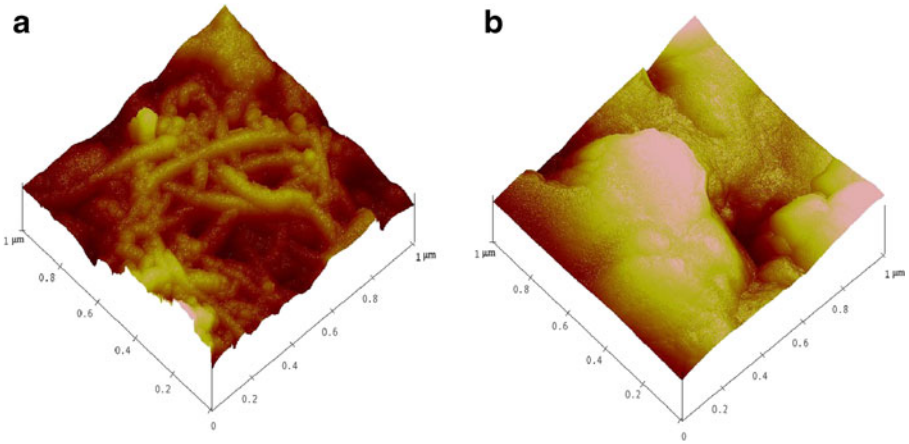

Fig. 2 AFM images of the PtNCs–MWNTs films (**a**) and GOX/PtNCs–MWNTs films (**b**) on the gold surface

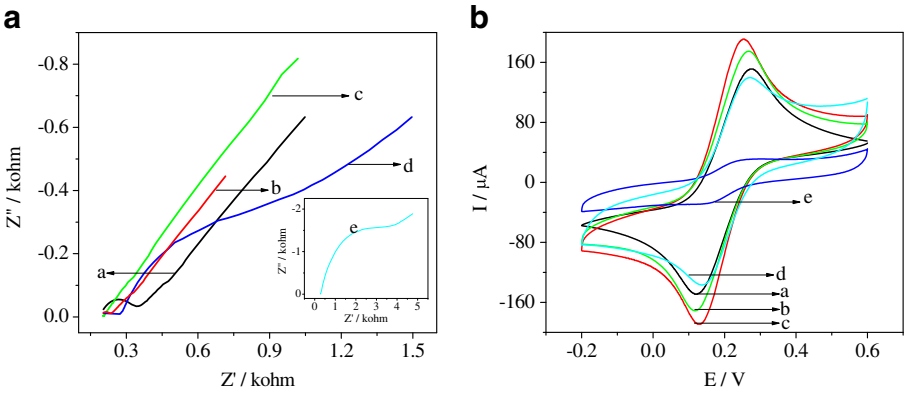

Fig. 3 EIS (**a**) and CVs (**b**) of the bare GCE (*a*), MWNTs/GCE (*b*), PtNCs–MWNTs/GCE (*c*), GOX/PtNCs–MWNTs/GCE (*d*), Nafion/GOX/PtNCs–MWNTs/GCE (*e*) in 5.0 mM $K_3[Fe(CN)_6]/K_4[Fe(CN)_6]$ (1:1). *Insert* of **a**: EIS of Nafion/GOX/PtNCs–MWNTs/GCE (*e*)

was observed when the electrode was modified with MWNTs (curve b). For the PtNCs–MWNTs composites-modified electrode, the EIS almost became a straight line (curve c). The lower R_{et} indicated that the PtNCs–MWNTs/GCE possessed more excellent conductive interface than MWNTs/GCE. Subsequently, the assembly of GOX generated an insulating layer on the electrode surface which functioned as a barrier to the interfacial electron transfer. This was reflected by the increased R_{et} (curve d). The resistance for the modified electrode increased again when non-conductive Nafion covered onto the GOX/PtNCs–MWNTs/GCE (Insert of Fig. 3a, curve e). These data show that PtNCs–MWNTs, GOX and Nafion were successfully assembled on the GCE surface.

Cyclic voltammetric (CV) experiment was used to evaluate the electrochemical performance of the electrodes. Figure 3b shows the CVs obtained for differently modified electrodes in 5.0 mM $K_3[Fe(CN)_6]/K_4[Fe(CN)_6]$ at the scan rate of 50 mV s^{-1}. There is a pair of well-defined redox peaks observed on the bare GCE with the anodic (E_{pc}) and cathodic (E_{pc}) peak potential of 0.271 and 0.121 V, respectively, and a peak to peak potential separation of 0.15 V (curve a). These peaks could be definitely attributed to the redox behaviors of $K_3[Fe(CN)_6]/K_4[Fe(CN)_6]$. After the electrode is modified with MWNTs, an obvious increase in reduction and oxidation peaks is observed (curve b), indicating the enhancing effect of MWNTs on the electric conductivity of the modified electrode. When PtNCs–MWNTs are immobilized onto GCE (curve c), the redox peak currents is apparently larger than that of the MWNTs/GCE. The result indicates that the PtNCs–MWNTs film is effectively immobilized on the GCE surface and provides the necessary conduction pathways. When GOX is embedded into the PtNCs–MWNTs film, the current response of CVs is inhibited, demonstrating that GOX prevents the diffusion of $K_3[Fe(CN)_6]/K_4[Fe(CN)_6]$ toward the electrode surface (curve d). Due to the non-conductive property of the Nafion, it could be observed that the redox peak currents decreased further after the modification of Nafion film (curve e). The results of the CV experiments could be well corroborated together with that of the impedance experiments for the characterization of electrode fabrication process.

Figure 4 shows the CVs of the modified electrode with the scan rate from 20 to 500 mV s^{-1}. With the increase of the scan rate, the redox peak currents increased simultaneously. As seen from the insert of Fig. 4, the peak current versus the scan rate plot was linear, which indicates that the kinetic behavior of the biosensor is of surface-confined [28].

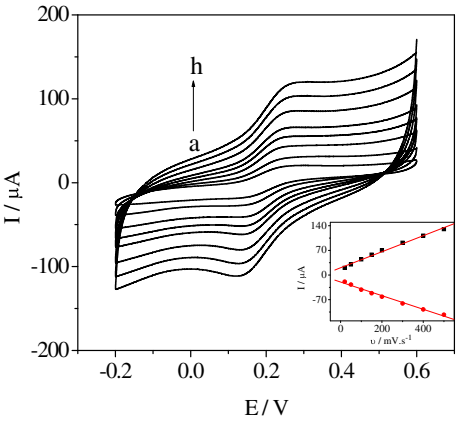

Fig. 4 CVs of the biosensor in 5.0 mM $K_3[Fe(CN)_6]/K_4[Fe(CN)_6]$ (1:1) at various scan rates. From *curves a* to *h* corresponding to 20, 50, 80, 100, 200, 300, 400 and 500 mV s^{-1}. *Inset*: The relationship between the peak currents and the scan rates

Detection of H_2O_2 at the PtNCs–MWNTs/GCE

According to Yang et al. [25], excellent electrocatalytic activity of the electrode toward H_2O_2 reveals that the electrode is able to provide a good signal transduction in the fabricated amperometric enzyme biosensors because H_2O_2 is the product of oxidase-based enzyme reactions.

The electrochemical behavior of the bare GCE, MWNTs/GCE and PtNCs–MWNTs/GCE in 0.1 M PBS (pH 7.0) with and without 2 mM H_2O_2 is shown in Fig. 5. As compared to the bare GCE (Fig. 5a, curve a), it is noted that the background current of the electrode increases after the MWNTs modification due to the high specific area of MWNTs (Fig. 5b, curve a). The background current of the PtNCs–MWNTs/GCE (Fig. 5c, curve a) is about three times higher than that of the MWNTs/GCE. After the addition of H_2O_2, no obvious change of the related CVs can be observed at the bare GCE (Fig. 5a, curve b). However, the oxidation current of H_2O_2 can be found obviously at both MWNTs/GCE (Fig. 5b, curve b) and PtNCs–MWNTs/GCE (Fig. 5c, curve b). Furthermore, the oxidation current of H_2O_2 at PtNCs–MWNTs is much higher than that at the MWNTs/GCE. This indicates that the PtNCs–MWNTs-modified electrode has higher electrocatalytic activity than the MWNTs–modified electrode. This is ascribed to the cooperation catalytic activity between PtNCs and MWNTs to H_2O_2.

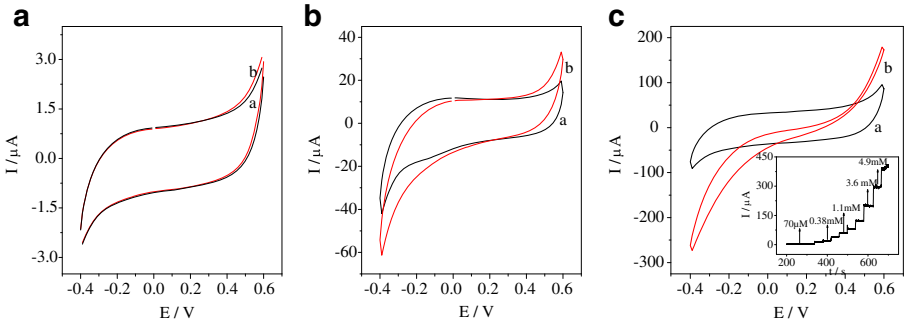

Fig. 5 CVs of the bare GCE (**a**), MWNTs/GCE (**b**) and PtNCs–MWNTs/GCE (**c**) in 0.1 M PBS without H_2O_2 (*a*) and with 2 mM H_2O_2 (*b*). Scan rate: 50 mV s^{-1}. *Insert*: Amperometric detection of H_2O_2 with the PtNCs–MWNTs/GCE in 0.1 M pH 7.0 PBS under stirring. Applied potential: 0.35 V

Chronoamperometry was employed to investigate the electrocatalytic ability towards the electrochemical oxidation of H_2O_2 at the PtNCs–MWNTs nanocomposites-modified GCE (the insert of Fig. 5c). When H_2O_2 was added into the PBS in series, the oxidation current increased steeply, which was ascribed to the good electrocatalytic activity of the PtNCs–MWNTs nanocomposites to H_2O_2 at the modified electrode. Hence, it is expected that the PtNCs–MWNTs nanocomposites can be applied to construct the biosensor which is based on the detection of H_2O_2.

Optimization of Experimental Parameters for the Biosensor

The influence of pH value of PBS on the amperometric response was measured, because the enzyme activity depends on the pH value of the testing solution. The pH effect was investigated over the range pH 5.0–8.5. Figure 6a shows the response of the biosensor against pH at a working potential of 0.35 V when the biosensor was subjected to 3.0 mM glucose at various pH of PBS. It can be seen that the amperometric responses increased with the increasing pH value from 5.0 to 7.0 and reached maximum at pH value of 7.0. A decrease in the amperometric response was observed when the pH value was over 7.0. Therefore, pH 7.0 of 0.1 M PBS was used for glucose determination in subsequent studies.

The effect of applied potential on the enzyme electrode response was studied in the range from 0 to 0.5 V in pH 7.0 PBS and the corresponding response current to 3.0 mM glucose is shown in Fig. 6b. The results demonstrate that the response current gradually increases with increasing positively applied voltage. A more positively applied voltage would lead to a higher sensitivity; however, it is preferable to control a lower applied voltage in order to avoid or decrease the interference caused by some coelectroactive species in the sample solution. Hence, working potential of 0.35 V was chosen for glucose determination in this work, where the biosensor could maintain reasonable sensitivity and reduce the interference caused by the electroactive species.

The Response Characteristics of the Biosensor

Due to the electrocatalytic activities of the PtNCs–MWNTs towards H_2O_2, an amperometric glucose biosensor was constructed by integration of GOX with the PtNCs–MWNTs. In the PBS, glucose is oxidized by the dissolved oxygen with the aid of the GOX and H_2O_2 is

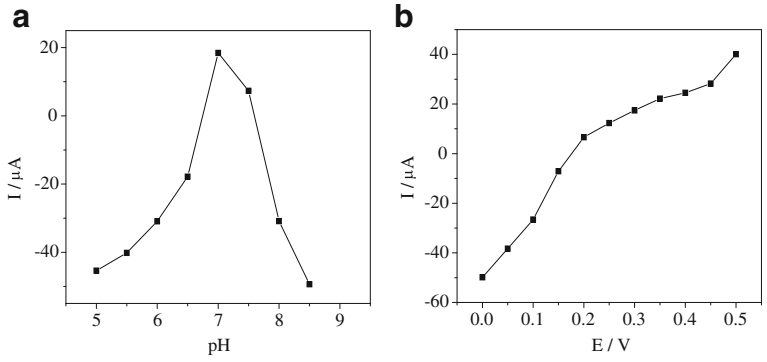

Fig. 6 Dependence of the current response of the biosensor to 3 mM glucose on the pH of PBS at an applied potential of 0.35 V (**a**) and on the applied potential in pH 7.0 PBS (**b**)

liberated during the course. The generated H_2O_2 is subsequently oxidized at the Nafion/GOX/PtNCs–MWNTs/GCE and gives rise to the anodic current which is directly proportional to the concentration of glucose. The whole process can be illustrated as the following reaction schemes:

$$\mathrm{GOX(FAD)} + \beta - \mathrm{D} - \mathrm{glucose} \rightarrow \mathrm{GOX(FADH_2)} + \beta - \mathrm{D} - \mathrm{gluconolactone} \quad (1)$$

$$\mathrm{GOX(FADH_2)} + \mathrm{O_2} \rightarrow \mathrm{GOX(FAD)} + \mathrm{H_2O_2} \quad (2)$$

$$\mathrm{H_2O_2} \xrightarrow{\mathrm{E}} 2\mathrm{H^+} + \mathrm{O_2} + 2\mathrm{e^-} \quad (3)$$

Figure 7 shows the CVs for the Nafion/GOX/PtNCs–MWNTs/GCE (Fig. 7a) and Nafion/GOX/MWNTs/GCE (Fig. 7b) recorded in PBS (pH 7.0, 0.1 M) in the absence (curve a) and presence (curve b) of 10 mM glucose. As observed in Fig. 7, upon the addition of glucose, the proposed biosensor (Nafion/GOX/PtNCs–MWNTs/GCE) exhibits much higher electrocatalytic activity towards the oxidation of glucose associated with increased anodic current, as compared to the Nafion/GOX/MWNTs/GCE. This result is consistent with the fact of the better electrocatalytic property of PtNCs–MWNTs than that of MWNTs. Firstly, the excellent electron-transfer ability of MWNTs improves the electrocatalytic activity of PtNCs–MWNTs. Secondly, the PtNCs–MWNTs-modified electrode possesses of high electroactive surface area, which is important for the electrocatalytic properties of PtNCs–MWNTs toward the oxidation of H_2O_2.

Figure 8a illustrates a typical current–time plot for the Nafion/GOX/PtNCs–MWNTs/GCE on successive additions of glucose at a working potential of 0.35 V. When an aliquot of glucose was added into the PBS, the oxidation current increased steeply along with glucose concentration. And the Nafion/GOX/PtNCs–MWNTs/GCE reached 95% of the steady-state current within 6 s. The rapid amperometric response of the biosensor could be owing to the highly conductive structure of PtNCs–MWNTs. The amperometric currents were measured at different concentrations of glucose and the calibration curves were obtained in Fig. 8b. The currents at the biosensor were proportional to the concentrations of glucose in the range from 3.0 μM to 12.1 mM, which extended over four orders of magnitude of glucose

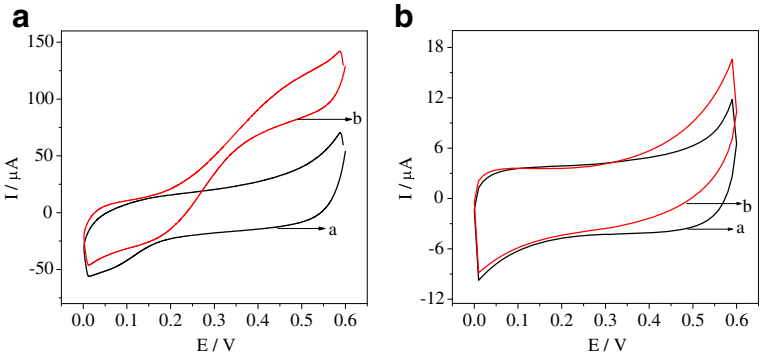

Fig. 7 CVs of Nafion/GOX/PtNCs–MWNTs/GCE (**a**) and Nafion/GOX/MWNTs/GCE (**b**) in 0.1 M PBS (pH 7.0) without glucose (*a*) and with 10 mM glucose (*b*). Scan rate: 50 mV s^{-1}

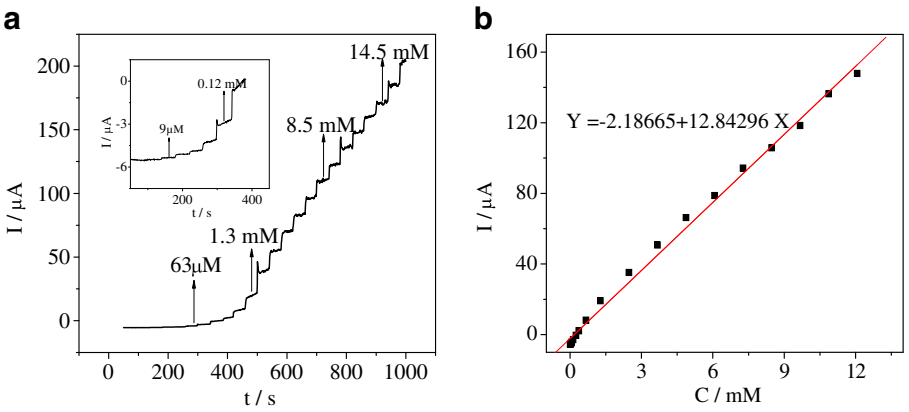

Fig. 8 **a** Amperometric response of the biosensor to glucose in a pH 7.0 PBS at an applied potential of 0.35 V upon successive additions of glucose at time intervals of 40 s. *Inset*: the magnification of amperometric response of the biosensor to glucose from 50 s to 400 s. **b**. The catalytic response current vs. glucose concentration

concentration, and it was much broader than 0.1–13.5 mM [17] and 1.0–7.0 mM [29] for adsorption of GOX at platinum nanoparticle-modified carbon nanotubes electrodes. A detection limit of 1.0 μM was obtained at S/N=3, which was about 50 times as low as 46.8 μM for GOX encapsulated in the films of CS–CdS/ACNTs–Pt_{nano} [30] and four hundred times as low as 0.4 mM for immobilization of GOX on Au_{nano}/Pt_{nano}/CNT electrode [23]. In the linear range, the Nafion/GOX/PtNCs–MWNTs/GCE has a high sensitivity of 12.8 μA mM^{-1}, which is about five times higher than 2.08 μA mM^{-1} [31], about twice higher than 4.49 μA mM^{-1} [32] and about 0.5 times higher than 8.53 μA mM^{-1} [33]. From these results, we can see that the proposed biosensor exhibits excellent performance in terms of wide linear range, low detection limit and good sensitivity, which may benefit from the huge surface area, favorable catalytic activity of PtNCs–MWNTs composites.

Apparent Michaelis–Menten Constant

When glucose concentration is saturated, a plateau current is observed, showing the characteristic of the Michaelis–Menten kinetics. The apparent Michaelis–Menten constant (K_m^{app}), an important parameter to reveal enzyme–substrate reaction kinetics, can be calculated according to the Lineweaver–Burk equation:

$$\frac{1}{I_{ss}} = \frac{K_m^{app}}{I_{max}} \times \left(\frac{1}{c_g}\right) + \frac{1}{I_{max}}$$

Here c_g is the substrate concentration, I_{ss} is the steady-state current and I_{max} is the maximum current measured under substrate saturation. From the curve of the $\frac{1}{I_{ss}}$ vs. $\frac{1}{c_g}$, the apparent Michaelis–Menten constant K_m^{app} was estimated to be 2.1 mM. The value of K_m^{app} is much lower than the reported values of K_m^{app} (7.9 mM [31], 10.73 mM [23] and 11.86 mM [30]) for other biosensors. These results show that the biosensor possesses high biological affinity to glucose.

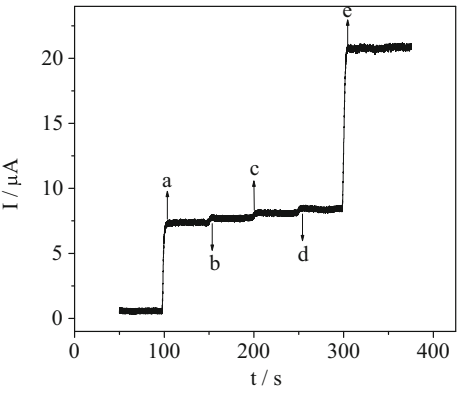

Fig. 9 Effect from the possible interferents on the glucose biosensor. Amperometric response of the biosensor to **a** 1 mM glucose, **b** 0.5 mM ascorbic acid, **c** 0.5 mM dopamine, **d** 0.5 mM L-cysteine and **e** 2 mM glucose in 0.1 M PBS at 0.35 V

Reproducibility, Stability and Anti-Interference of the Biosensor

The reproducibility of enzyme electrode was estimated from the response to 3.0 mM glucose at five enzyme electrodes prepared under the same experimental conditions. The results reveal that the biosensor has satisfied reproducibility with a relative standard deviation of 7.5%.

The stability of the resulted electrodes was evaluated by tracing the sensitivity of the electrode response ever 2 days. When not in use, the electrode was suspended above 0.1 M PBS at 4 °C in a refrigerator, and it maintained over 80% of the initial value in the response to 3.0 mM glucose after a month. The decrease in current response may be due to denaturation of the enzyme. The good stability can be attributed to the following aspects. On the one hand, the fabrication process is mild and no damage is made on the enzyme molecule. On the other hand, PtNCs–MWNTs possesses good biocompatibility that could retain the bioactivity of the enzyme molecule.

The proposed biosensor is capable of reducing the interferences caused by the substances such as ascorbic acid, dopamine and L-cysteine. Figure 9 shows the effects of ascorbic acid, dopamine and L-cysteine on the response current to glucose. The interference tests were carried at 0.35 V in the presence of 0.5 mM ascorbic acid, 0.5 mM dopamine, 0.5 mM L-cysteine, when 1 mM glucose was contained in a 0.1 M PBS (pH 7.0). The observed current responses to the additions of ascorbic acid, dopamine and L-cysteine were very small, in vivid contrast to the large response to glucose. The results suggest that the effects of electroactive interferents on the response current are really not obvious at the applied potential in the case of the existence of Nafion. Hereby, we can conclude that the resulting biosensor has a strong anti-interference ability.

Table 1 Determination of glucose in blood serum samples

Serum sample	Determined by 9th People's Hospital (mM)	Determined by current method[a] (mM)	RSD (%)	Relative deviation (%)	Glucose added (mM)	Glucose founded[a] (mM)	Recovery (%)
1	5.00	5.10±0.10	2.0	2.0	3.00	2.94±0.12	98.0
2	6.00	6.26±0.15	2.4	4.3	3.00	2.99±0.08	99.7
3	9.70	9.34±0.44	4.7	−3.7	3.00	3.05±0.16	101.7

[a] Average value from three determinations

Human Serum Sample Analysis

In order to verify the analytical applicability of the biosensor, it was applied to the determination of glucose in human blood serum. The glucose concentration of three serum samples was analyzed by the glucose biosensor. As can be seen from Table 1, the results were satisfactory and agree closely with those measured by the biochemical analyzer in the hospital. Analytical recoveries of the glucose solution added to blood serum samples were from 98.0% to 101.7%. The satisfying results demonstrate that the biosensor has a great potential for practical application.

Conclusions

The large specific surface area, high conductivity and excellent elelctroactivity of the PtNCs–MWNTs nanocomposites enable it to be used as an outstanding matrix for enzyme immobilization and electrocatalysis. In this paper, glucose oxidase (GOX), as a model enzyme, was immobilized on the PtNCs–MWNTs nanocomposites to achieve a biosensor. The detection limit of the proposed biosensor is as low as 1.0 μM, linear range is as wide as 3.0 μM–12.1 mM and sensitivity is as high as 12.8 μA mM^{-1} for the determination of glucose. Besides the characteristics above, the resulting biosensor also has a strong anti-interference ability and shows a satisfactory reproducibility and stability. This method can be used in the preparation of other amperometric enzyme biosensors. The satisfying results for serum sample analysis demonstrate that the biosensor has a great potential for practical application.

Acknowledgments This work was supported by the National Natural Science Foundation of China (21075100), Key Lab of Chongqing Modern Analytical Chemistry (201004), the Doctor Foundation of Southwest University (SWUB2008048) and the Fundamental Research Funds for the Central Universities (XDJK2009C082).

References

1. Liu, X. Q., Shi, L. H., Niu, W. X., Li, H. J., & Xu, G. B. (2008). Amperometric glucose biosensor based on single-walled carbon nanohorns. *Biosensors and Bioelectronics, 23*, 1887–1890.
2. Fu, Y. C., Chen, C., Xie, Q. J., Xu, X. H., Zou, C., Zhou, Q. M., Tan, L., Tang, H., Zhang, Y. Y., & Yao, S. Z. (2008). Immobilization of enzymes through one-pot chemical preoxidation and electropolymerization of dithiols in enzyme-containing aqueous suspensions to develop biosensorswith improved performance. *Analytical Chemistry, 80*, 5829–5838.
3. Sljukic, B., Banks, C. E., Salter, C., Crossley, A., & Compton, R. G. (2006). Electrochemically polymerised composites of multi-walled carbon nanotubes and poly(vinylferrocene) and their use as modified electrodes: Application to glucose sensing. *Analyst, 131*, 670–677.
4. Ballerstadt, R., Kholodnykh, A., Evans, C., Boretsky, A., Motamedi, M., Gowda, A., & McNichols, R. (2007). Affinity-based turbidity sensor for glucose monitoring by optical choherence tomography: Toward the development of an implantable sensor. *Analytical Chemistry, 79*, 6965–6974.
5. Diem, P., Kalt, L., Haueter, U., Krinelke, L., Fajfr, R., Reihl, B., & Beyer, U. (2004). Clinical performance of a continuous viscometric affinity sensor for glucose. *Diabetes Technology & Therapeutics, 6*, 790–799.
6. Malitesta, C., Losito, I., & Zambonin, P. G. (1999). Molecularly imprinted electrosynthesized polymers: New materials for biomimetic sensors. *Analytical Chemistry, 71*, 1366–1370.
7. Chuang, C. W., & Shih, J. S. (2001). Preparation and application of immobilized C_{60}-glucose oxidase enzyme in flullerence C_{60}-coated piezoelectric quartz crystal glucose sensor. *Sensors and Actuators B-Chemical, 81*, 1–8.

8. Gallego, R. G., Haseley, S. R., van Miegem, V. F. L., Vliegenthart, J. F. G., & Kamerling, J. P. (2004). Identification of carbohydrates binding to lectins by using surface plasmon resonance in combination with HPLC profiling. *Glycobiology, 14*, 373–386.
9. Shi, Q. F., Han, E., Shan, D., Yao, W. J., & Xue, H. G. (2008). Development of a high analytical performance amperometric glucose biosensor based on glucose oxidase immobilized in a composite matrix: Layered double hydroxides/chitosan. *Bioprocess and Biosystems Engineering, 31*, 519–526.
10. Li, F., Feng, Y., Yang, L. M., Li, L., Tang, C. F., & Tang, B. (2011). A selective novel non-enzyme glucose amperometric biosensor based on lectin–sugar binding on thionine modified electrode. *Biosensors and Bioelectronics, 26*, 2489–2494.
11. Xu, Y., & Lin, X. (2007). Selectively attaching Pt-nano-clusters to the open ends and defect sites on carbon nanotubes for electrochemical catalysis. *Electrochimica Acta, 52*, 5140–5149.
12. Welch, C. M., & Compton, R. G. (2006). The use of nanoparticles in electroanalysis: A review. *Analytical and Bioanalytical Chemistry, 384*, 601–619.
13. Raimondi, F., Scherer, G. G., Kötz, R., & Wokaun, A. (2005). Nanoparticles in energy technology: Examples from electrochemistry and catalysis. *Angewandte Chemie International Edition, 44*, 2190–2209.
14. Lin, Y., & Finke, R. G. (1994). Novel polyoxoanion- and Bu_4N^+-stabilized, isolable, and redissolvable, 20-30-.ANG. Ir300-900 nanoclusters: The kinetically controlled synthesis, characterization, and mechanism of formation of organic solvent-soluble, reproducible size, and reproducible catalytic activity metal nanoclusters. *Journal of the American Chemical Society, 116*, 8335–8353.
15. Li, W. J., Yuan, R., Chai, Y. Q., & Chen, S. H. (2010). Reagentless amperometric cancer antigen 15–3 immunosensor based on enzyme-mediated direct electrochemistry. *Biosensors and Bioelectronics, 25*, 2548–2552.
16. Zhao, Z. W., Chen, X. J., Tay, B. K., Chen, J. S., Han, Z. J., & Khor, K. A. (2007). A novel amperometric biosensor based on ZnO:Co nanoclusters for biosensing glucose. *Biosensors and Bioelectronics, 23*, 135–139.
17. Balasubramanian, K., & Burghard, M. (2006). Biosensors based on carbon nano-tubes. *Analytical and Bioanalytical Chemistry, 385*, 452–468.
18. Xiong, W., Du, F., Liu, Y., Perez, A. J., Supp, M., Ramakrishnan, T. S., Dai, L. M., & Jiang, L. (2010). 3-D Carbon nanotube structures used as high performance catalyst for oxygen reduction reaction. *Journal of the American Chemical Society, 132*, 15839–15841.
19. Iijiman, S. (1991). Helical microtubules of graphitic carbon. *Nature, 354*, 56–58.
20. Wang, J., Gu, M., Di, J., Gao, Y., Wu, Y., & Tu, Y. (2007). A carbon nanotube/silica sol–gel architecture for immobilization of horseradish peroxidase for electrochemical biosensor. *Bioprocess and Biosystems Engineering, 30*, 289–296.
21. Ishikawa, F. N., Stauffer, B., Caron, D. A., & Zhou, C. W. (2009). Rapid and label-free cell detection by metal-cluster-decorated carbon nanotube biosensors. *Biosensors and Bioelectronics, 24*, 2967–2972.
22. Lordi, V., Yao, N., & Wei, J. (2001). Method for supporting platinum on single-walled carbon nanotube for a selective hydrogenationcatalyst. *Chemistry of Materials, 13*, 733–737.
23. Chu, X., Duan, D. X., Shen, G. L., & Yu, R. Q. (2007). Amperometric glucose biosensor based on electrodeposition of platinum nanoparticles onto covalently immobilized carbon nanotube electrode. *Talanta, 71*, 2040–2047.
24. Li, J. J., Yuan, R., Chai, Y. Q., & Che, X. (2010). Fabrication of a novel glucose biosensor based on Pt nanoparticles-decorated iron oxide-multiwall carbon nanotubes magnetic composite. *Journal of Molecular Catalysis B: Enzymatic, 66*, 8–14.
25. Yang, M. H., Yang, Y. H., Liu, Y. L., Shen, G. L., & Yu, R. Q. (2006). Platinum nanoparticles-doped sol–gel/carbon nanotubes composite electrochemical sensors and biosensors. *Biosensors and Bioelectronics, 21*, 1125–1131.
26. Lin, Y. H., Cui, X. L., Yen, C., & Wai, C. M. (2005). Platinum/carbon nanotube nanocomposite synthesized in supercritical fluid as electrocatalysts for low-temperature fuel cells. *The Journal of Physical Chemistry. B, 109*, 14410–14415.
27. Kim, S., Jung, Y., & Park, S. J. (2008). Preparation and electrochemical behaviors of platinum nanocluster catalysts deposited on plasma-treated carbon nanotube supports. *Colloids and Surfaces A, 313–314*, 189–192.
28. Liu, Y., Wang, M. K., Zhao, F., Xu, Z. A., & Dong, S. J. (2005). The direct electron transfer of glucose oxidase and glucose biosensor based on carbon nanotubes/chitosan matrix. *Biosensors and Bioelectronics, 21*, 984–988.
29. Wen, D., Zou, X. Q., Liu, Y., Shang, L., & Dong, S. J. (2009). Nanocomposite based on depositing platinum nanostructure onto carbon nanotubes through a one-pot, facile synthesis method for amperometric sensing. *Talanta, 79*, 1233–1237.

30. Yang, J., Zhang, R. Y., Xu, Y., He, P. G., & Fang, Y. Z. (2008). Direct electrochemistry study of glucose oxidase on Pt nanoparticle-modified aligned carbon nanotubes electrode by the assistance of chitosan–CdS and its biosensoring for glucose. *Electrochemistry Communications, 10*, 1889–1892.
31. Kang, X. H., Mai, Z. B., Zou, X. Y., Cai, P. X., & Mo, J. Y. (2008). Glucose biosensors based on platinum nanoparticles-deposited carbon nanotubes in sol–gel chitosan/silica hybrid. *Talanta, 74*, 879–886.
32. Yuan, L., Yang, M. H., Qu, F. L., Shen, G. L., & Yu, R. Q. (2008). Seed-mediated growth of platinum nanoparticles on carbon nanotubes for the fabrication of electrochemical biosensors. *Electrochimica Acta, 53*, 3559–3565.
33. Kang, X. H., Mai, Z. B., Zou, X. Y., Cai, P. X., & Mo, J. Y. (2007). A novel glucose biosensor based on immobilization of glucose oxidase in chitosan on a glassy carbon electrode modified with gold–platinum alloy nanoparticles/multiwall carbon nanotubes. *Analytical Biochemistry, 369*, 71–79.